Heliyon 10 (2024) e37401

Contents lists available at ScienceDirect

Heliyon

journal homepage: www.cell.com/heliyon

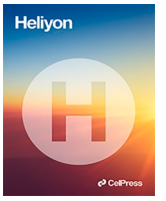

Research article

Nitrogen mustard induces dynamic nuclear protein spectrum change and DNA-protein crosslinking, with p97 mediating repair

Jin Cheng [a,b,*], Haoyin Liu [a], Wenpei Yu [a], Xunhu Dong [a], Yan Sai [a], Feng Ye [a], Guorong Dan [a], Mingliang Chen [a], Yuanpeng Zhao [a], Xi Zhang [a], Zhongmin Zou [a,**]

[a] Department of Chemical Defense Medicine, School of Preventive Medicine, The Third Military Medical University Army Medical University, Chongqing, China
[b] Department of Clinic, Chongqing Medical and Pharmaceutical College, Chongqing, China

ARTICLE INFO

Keywords:
Proteomics
DNA-Protein cross-linking
Nitrogen mustard
Nucleus
p97

ABSTRACT

Nitrogen mustard (NM) is a chemotherapeutic agent capable of alkylating nucleophilic proteins and DNA, causing severe cell damage. However, no reports have been on the dynamic changes in proteomics induced by NM. In this study, we established a model of acute exposure to NM for 1 h and a continuous cultured model for 24 h after NM removal (repair stage) using 16HBE cells. The nuclear protein spectrum and nuclear proteins crosslinked with DNA were analyzed, and the function of p97 during NM damage was examined. An hour of NM exposure resulted in severe changes in the nuclear protein spectrum and protein into the cell nucleus, which is mainly involved in nuclear acid-related issues. After 24 h, the return to normal process of the types and amounts of differentially expressed proteins was inhibited by si-p97. The main processes involved in si-p97 intervention were nucleocytoplasmic transport, processing in the endoplasmic reticulum, metabolic abnormalities, and DNA-response; however. An hour of exposure to NM increased DNA-protein crosslinking (DPC), total-H2AX, and p-H2AX. In contrast, si-p97 only further increased or maintained their levels at 24 h yet not at 1 h. The effect of the proteasome inhibitor, MG132, was similar to that of si-p97. The siRNA of DVC1, a partner of p97, also increased the DPC content. Both si-p97 and si-DVC1 increased the cytoplasmic levels of the proteasome (PSMD2). These results suggest acute NM exposure induces severe nuclear protein spectral changes, rapid protein influx into the nucleus, DPC formation, and DNA double-strand breaks. Furthermore, our data indicated that p97 is involved in normal protein spectrum maintenance and DPC removal after NM withdrawal, requiring the participation of DVC1 and the proteasome.

1. Introduction

Nitrogen mustard (NM) was initially designed as a potential chemical warfare agent but was later found to be useful in cancer treatment [1]. It is highly toxic to normal tissues, causing inflammatory damage to the respiratory system, skin, and eyes [2,3]. In the

* Corresponding author. Department of Chemical Defense Medicine, School of Preventive Medicine, The Third Military Medical University Army Medical University, Chongqing, China.
** Corresponding author.
E-mail addresses: chengjin09@qq.com (J. Cheng), zmzou@tmmu.edu.cn (Z. Zou).

https://doi.org/10.1016/j.heliyon.2024.e37401
Received 29 March 2024; Received in revised form 1 September 2024; Accepted 3 September 2024
Available online 4 September 2024

Abbreviations

NM	Nitrogen mustard
BAA	Bifunctional alkylating agent
DPC	DNA-protein cross-link
DSB	Double-strand break

20th century, NM became the cornerstone of anticancer chemotherapy and remains significant today [1,4]. NM is a bifunctional alkylating agent (BAA) with two active electrophilic alkyl groups [5], namely, active N-chloroethyl groups, that can react with nucleophilic groups in DNA or proteins [6,7], causing severe damage through genetic and cellular toxicity.

Proteins are major target molecules in NM-induced damage [7] and serve as key indicators of cellular status. NM can directly cross-link proteins to DNA, forming DNA-protein crosslinks (DPC), a type of DNA damage [8]. However, the extensive alkylation of protein nucleophilic groups induced by NM can cause cellular microenvironment damage, as well as various stress responses such as inflammation [9] and oxidative damage [10–13]. Thus, monitoring the changes in the protein spectrum can provide a macroscopic and dynamic understanding of NM-induced damage. However, the alterations in the protein spectrum during the progression of NM-induced damage remain unclear.

When NM damage occurs, a substantial number of proteins may be damaged, and nuclear proteins may further cross-link with DNA, indirectly exacerbating errors in DNA replication, transcription, and protein translation [14,15]. Therefore, transporting and degrading a large number of proteins to alleviate the damage caused by DPC and mitigate the stress responses that disrupt cellular homeostasis is warranted. p97 (also known as VCP, Cdc48, or Ter94) belongs to the functionally diverse AAA + superfamily of proteins (ATPases associated with various cellular activities) superfamily of proteins [16]. p97 regulates protein homeostasis, membrane fusion, vesicle transport, and chromatin-related functions in various cellular pathways [17]. p97 extracts and/or disassembles ubiquitinated substrates from membranes, chromatin, and large protein complexes [16,18]. However, the role of p97 in the repair of NM-induced damage has not been reported.

In the present study, we hypothesized that p97 plays a crucial role in NM damage repair. To validate this hypothesis, we investigated the nuclear protein spectrum after NM damage, focusing on temporal changes in nuclear proteins and the role of p97 in alterations of the nuclear protein spectrum and DPC content after damage. Our results indicate that NM induces a significant change in the nuclear protein spectrum, causing an influx of proteins into the cell nucleus and the formation of DPC with DNA during the early exposure phase. P97 facilitates protein transportation and elimination of DPC and plays a crucial role in the later stages of cellular repair. The repair function of p97 appears to be closely associated with the proteasome and DVC1 function.

2. Materials and methods

2.1. Cell culture and treatment

The human bronchial epithelial cell line 16HBE (RRID: CVCL_0112) was purchased from American Type Culture Collection (ATCC). The cell line was identified by Short Tandem Repeat (STR) authentication prior to the start of the experiment and submission, and no mycoplasma was detected by PCR. The cell line was cultured in MEM containing 10 % fetal bovine serum (FBS). Approximately $1 \times 10\hat{}7$ cells were seeded in each 100 mm culture dish and maintained in a humidified atmosphere at 37 °C with 5 % CO_2/95 % air. When the cell density was 70–80 %, the cells were treated with NM (DB, China) freshly dissolved in PBS. The concentration of NM in the culture medium was 50 μM. Cells were incubated in an NM-containing medium for 1 h, after which half of the cells were collected, and the other half were cultured in a normal medium for an additional 24 h. For proteasome inhibition, 2 μM of the proteasome inhibitor MG132 (Selleck Chemicals, Houston, TX, USA) was added, and cells were incubated for 3 h before being transferred to normal culture medium.

2.2. Transient transfection

Approximately $1 \times 10\hat{}7$ cells were seeded in each 100 mm cell culture dish. The next day, synthetic DVC1 and p97 siRNAs (Invitrogen Corp., Waltham, MA, USA) were transfected into cells using Lipofectamine 2000 (Invitrogen Corp.) according to the manufacturer's protocol. Cells were treated with NM in the same manner as described above within 2 days after transfection.

2.3. Metabolite extraction and targeted LC-MS (liquid Chromatograph mass spectrometer) analysis

Targeted LC-MS analysis of the samples was performed using the BIOTREE software (Shanghai, China). Cells with or without NM or si-p97 were collected and nuclear proteins were separated using a nuclear and cytoplasmic protein extraction kit (Beyotime, China). The proteins were adjusted to the same concentration and digested into peptides using trypsin. After assessing the efficiency of the enzymatic digestion, the peptides were labeled with TMT6. Samples subjected to different treatments were labeled with isotopes of different sizes. The labeled peptides were desalted and deionized using a desalting column and acetonitrile, and subsequently separated under high pH conditions. MS (Orbitrap Fusion) was used to detect the peptides and Proteome Discoverer (PD) (version

2.4.0.305, Thermo Fisher Scientific) was used for spectrum filtering. The Sequest HT search engine and UniProtKB-SwissProt databases were used for spectrum analysis.

2.4. DPC separation

The DPC separation was performed following the protocol described by Kiianitsa [19] with some modifications. Briefly, the cells were dissolved by adding DNAiso reagent (TaKaRa Bio Inc., Japan) to the solution (not exceeding 2 × 10^6 cells per 1 ml). After 5 min, the nucleic acids and DPC were precipitated by adding 0.5 vol of 100 % ethanol, followed by centrifugation, and the pellet was washed twice with 75 % ethanol. After ethanol evaporation, the pellet was resuspended in TE buffer or Milli-Q water and the DNA concentration was quantified.

2.5. Quantification of DNA and protein in DPC Preparation

SYBR Green binds to double-stranded DNA (dsDNA), and the amount of dsDNA is proportional to the intensity of the emitted fluorescence. Bovine thymus standard DNA (Sigma-Aldrich, St. Louis, MO, USA) was diluted to a final concentration range of 0.5 ng/μL to 8 ng/μL using TE for serial dilution. Subsequently, DPC samples collected from 100 mm culture dishes were diluted to 1:1000. One hundred microliters of bovine thymus DNA or DPC samples were added to each well of a 96-well plate, followed by the addition of an equal volume of SYBR Green solution (Rebio Tech. Ltd., China). After 15 min of incubation in the dark, the fluorescence intensity was measured, and the DNA concentration of DPC samples was calculated based on a standard curve generated using bovine thymus DNA [20].

For protein quantification, a fluorescein isothiocyanate (FITC) stock solution was added to the DPC solution (10 μg) to achieve a final FITC concentration of 0.1 mM. The solution was incubated at room temperature for 1 h to label the cross-linked proteins. The labeled DPC were precipitated with 100 % ethanol, washed twice with 75 % ethanol, air-dried, and dissolved in Tris-EDTA (TE) buffer. Fluorescence intensity was measured using a fluorescence spectrometer to quantify the levels of FITC-labeled proteins. The loading amount of the DPC samples can be adjusted based on the protein concentration [21].

For the immunological detection of DPC, equal amounts of DNA samples were slot-blotted onto a nitrocellulose membrane under vacuum and washed three times with TBS. The membrane was blocked with 1 % BSA and incubated with an anti-FITC primary antibody (Sigma-Aldrich, USA). The membrane was incubated with an ECL substrate, and luminescent images were captured with Fusion Fx and FusionCapt Advance.

2.6. GST Pull-down

The DVC1 plasmid was cloned into the pet-GST vector (GeneCreate, China), expressed, and purified as GST-DVC1 protein in the Escherichia coli system. GST-DVC1 and a negative control (GST) were incubated with protein samples from cell lysates of different treatment groups along with agarose beads. SDS-PAGE was performed on the washed solutions from each group and Western blotting was performed using a rabbit polyclonal anti-GST antibody (Santa Cruz Biotechnology, Dallas, Texas, USA). Mass spectrometry was used to identify the bound proteins if GST-fused proteins were detected.

2.7. Western blot

The method was performed using nitrocellulose membranes following standard procedures. Rabbit polyclonal anti-p97 antibody (Abcam, Cambridge, Massachusetts, USA), rabbit polyclonal anti-p-H2AX antibody (Santa Cruz Biotech., USA), and mouse polyclonal anti-β-actin antibody (Santa Cruz Biotech., USA) were all used at a dilution of 1:1000. The bands were captured and their intensity was quantified. Band intensities of target proteins were adjusted by calculating the ratio to β-actin.

2.8. Immunofluorescence

Cells were washed with PBS and treated with 4 % paraformaldehyde and 0.5 % Triton X. Nonspecific binding was blocked with goat serum, followed by overnight incubation with rabbit polyclonal anti-PMSD2 antibody (CST, USA). The next day, FITC-labeled rabbit anti-rabbit secondary antibody was added and the cell nuclei were stained with DAPI.

2.9. Proteasome activity assay

To assess the activity of the 20S proteasome, 7-amino-4-methylcoumarin (AMC) was diluted to different concentrations (from 12.5 μM to 0.20 μM) to create a standard curve. Protein samples collected from cell lysates were adjusted to the same concentrations. The proteasome substrate (Suc-LLVY-AMC) was added to the same amount of the protein sample to generate AMC. The fluorescence intensity of AMC was detected at 380/460 nm and the inhibition rate of proteasome activity was calculated from the standard curve.

2.10. Statistical analysis

For LC-MS analysis, three parallel samples were mixed and the Significance B algorithm [22] was used to filter different proteins.

Metabolic pathway analyses were conducted using the Kyoto Encyclopedia of Genes and Genomes (KEGG) pathway database (www.kegg.jp/kegg/pathway.html). Other experimental data were analyzed by one-way analysis of variance and presented as mean ± standard deviation. Subsequent tests were performed using the Bonferroni correction. Statistical significance was set at P-value <0.05.

3. Result

3.1. Acute NM exposure induces changes in the composition of nuclear proteins, and p97 predominantly assists in the extrusion of proteins from the nucleus at later period

Cellular damage and repair are dynamic processes; therefore, we focused on the differences in protein expression at various time points after NM exposure to reflect the performance of cells at different time intervals. As NM exposure typically leads to acute injury and cell death, we used 1 h of continuous NM treatment to induce early cell damage. Subsequently, the cells were cultured for 24 h in a normal culture medium after NM treatment, simulating the self-repair of cells after exposure. Nuclear protein changes were the focus of the following experiment and were described using targeted LC-MS analysis.

The relative expression levels of nuclear proteins in the control and NM treatment groups were calculated. Differentially expressed nuclear proteins ($P < 0.05$) whose fold changes were more than 1.2 times or less than 0.83 time compared to the control were collected (Fig. 1A, and the blue, green, and purple dots in 1B). In total, 448 nuclear proteins were upregulated after 1 h of NM treatment, which decreased to 308 after 24 h, and the protein spectra of the two treatiments coincided less (Fig. 1C). The results indicate that the nuclear protein profile changed significantly from 1 to 24 h. Many proteins entered and exited the nucleus, and the degree of entry and exit was more pronounced at 1 h. After NM exposure, the number of downregulated nuclear proteins did not differ significantly at 24 h (318 vs. 328). However, the protein profiles coincided less, which indicated a significant content change but a comparable intensity (Fig. 1D).

Treatment with NM + si-p97 exacerbated the upregulation of nuclear proteins at 1 and 24 h (Fig. 1C). In addition, the number of downregulated nuclear proteins in the NM + si-p97 group increased significantly at 24 h compared to 1 h (335 vs. 258) (Fig. 1D). These results suggest that the deletion of p97 mainly affected the recovery of the protein spectrum to normal during the later stage of cell repair, because the number of differentially expressed proteins can partly reflect the degree of change compared to the normal state.

Although Fig. 1C and D showed that a greater variety of proteins were altered in the nucleus following NM treatment, both with and without si-p97, this does not necessarily indicate an increase in the overall protein content. Therefore, we tested whether severe nucleic changes were associated with increased protein quantities. The ratio of nuclear protein to total protein was calculated. At 1 h and 24 h, the protein content in the nucleus of the NM group was higher than that in the normal control group. Si-p97 elevated this level at 24 h, but not at 1 h (Fig. 1E). This suggests that during the repair process after NM exposure, si-p97 inhibits the transfer of a larger number of proteins out of the cell nucleus in addition to a greater variety of proteins.

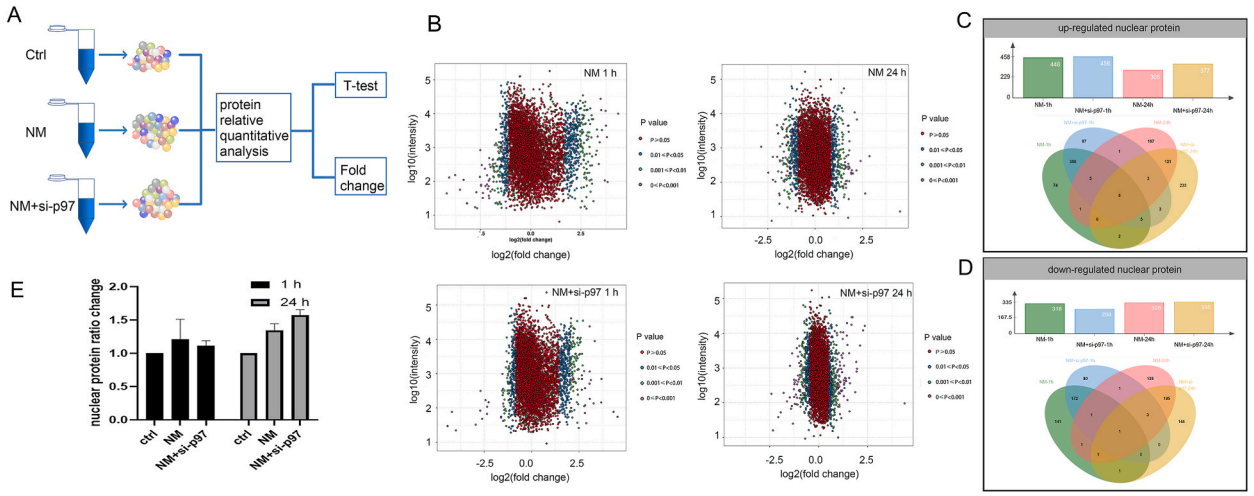

Fig. 1. Impact of NM exposure and si-p97 intervention on protein spectrum and amount in the cell nucleus. (A) Schematic diagram of the quantitative detection steps for tandem mass spectrometry-labeled protein groups. Nuclear proteins were extracted from three processed samples, and their expression differences were quantitatively analyzed. (B) Dynamic profiles of nuclear proteins 1–24 h after NM treatment with or without si-p97 intervention. The expression levels of nuclear proteins in the NM group and si-p97+NM group were compared with the control group, with the x-axis representing the multiple changes in protein (log2-based) and the y-axis representing the information on protein expression levels (log10-based). Blue ($0.01 \leq P < 0.05$), green ($0.001 \leq P < 0.01$), and purple dots ($P < 0.001$) represent the significant screening results with fold change ≥ 1.2 or ≤ 0.83, while non-significant proteins ($P \geq 0.05$) are shown in red. (C, D) Histogram and Venn diagram showing the number of up-regulated or down-regulated nuclear proteins in NM and NM + si-p97 groups at 1 h and 24 h, respectively. (E) Changes in the ratio of nuclear proteins to total proteins in NM and si-p97+NM groups at different time points. The adjustment was made by setting the ratio of nuclear proteins to total proteins in the control group as 1.

3.2. Acute NM exposure affects upstream **protein synthesis and substance metabolism processes**, and p97 deficiency hinders nucleocytoplasmic transport

Venn diagrams were used to filter out nuclear proteins with changes in expression after NM, si-p97, and si-p97+NM treatments to further understand the differential expression of nuclear proteins. After 1 h of NM exposure, 171 proteins showed changes under all three treatment conditions (middle overlap in Fig. 2Ai), indicating that the expression of these nuclear proteins was significantly altered by NM, si-p97, or si-p97+NM. Separating nuclear proteins into upregulated and downregulated subgroups, the middle overlap in Fig. 2Aii indicated that si-p97 further exacerbated the effects of NM on five nuclear proteins (GFPT2, RSPH3, FSHR, BMP3, and IZUMO2) (Fig. 2Aiv). Similarly, the middle overlap in Fig. 2Aiii indicated that si-p97 further exacerbated the effects of NM on four nuclear proteins (MGST1, SREBF1, TMEM19, and TRMT112) (Fig. 2Av). These nine proteins are related to cell metabolism, suggesting that p97 deficiency exacerbates the damage to cell metabolism caused by NM at 1 h.

We further performed a clustering analysis of all differentially expressed nuclear proteins based on KEGG to confirm the biological functions of significantly different proteins. We ranked the cellular signaling pathways by gene ratio. After 1 h of NM exposure, regardless of the presence of si-p97, the top three pathways involved were spliceosome, ribosome biogenesis in eukaryotes, and the mRNA surveillance pathway (Fig. 2B). This suggests that NM, and not p97, predominantly influences these pathways. Active DNA transcription, mRNA accuracy checking, and new protein synthesis are the predominant changes that occur during the early stages of NM damage. We subsequently distinguished the nuclear proteins into upregulated and downregulated subgroups. We observed that for the upregulated proteins, due to the undetection of four proteins (DDX39B, ALYREF, NUP35, and GLE1) (Supplementary Table 1), the nucleocytoplasmic transport pathway was less significant in the NM + si-p97 group than in the NM group (Fig. 2C). These four proteins are associated with protein splicing transport, central channels, and endoplasmic reticulum fibers, suggesting that p97 deficiency affects these functions during acute NM injury. The metabolic pathway was the most inhibited for the downregulated proteins at 1 h (Fig. 2D), indicating direct and rapid inhibition of energy production during this period, which was slightly more severe when si-p97 was added. Other pathways involved in Fig. 2D were mainly related to substance metabolism, with a slight difference after si-p97 intervention.

3.3. Endoplasmic reticulum-related protein transport was the main task during the cellular repair phase after NM exposure; si-p97 affects the transportation and DNA repair manner

After 1 h of treatment, the normal culture medium was replaced with a medium containing NM, and the cells were cultured for 24 h. This approach was used to reflect the repair phase after NM exposure. A total of 52 nuclear proteins (the middle overlapping portion in Fig. 3Ai) were significantly altered by NM, si-p97, or si-p97+NM. Subsequently, we divided all the differentiated nuclear proteins into upregulated and downregulated subgroups. The overlap in the middle of Fig. 3Aii indicated that si-p97 further intensified the effect of NM on 18 proteins' upregulation (Fig. 3Aiv); (H2AX, MRM3, H2BC13, HIST3H2A, AREG, APOE, LAMP2, HIST2H2AC, HBA1, HIST2H2AB, ATF3, S100A9, IGLC2, SNAPC4, LYZ, GPX3, ANP32C, and RPIA). Similarly, the overlap in the middle of Fig. 3Aiii indicates that si-p97 further intensified the effect of NM on 11 proteins' downregulation (EHD2, PDK1, CRIP2, CLP1, MT-ND4, ANGPTL4, IREB2, KAT8, TOR1AIP2, SLC25A15, and SLC35F6) (Fig. 3Av).

We also clustered the differentially expressed nuclear proteins 24 h after NM treatment and identified the top 10 signaling pathways based on the gene ratio. After a period of repair at 24 h, the predominant pathway was protein processing in the endoplasmic reticulum, indicating that this was a major task during this stage. However, compared to the NM treatment alone, the addition of si-p97 made the enrichment of this pathway less significant. The nine pathways involved were associated with the metabolism of various substances (Fig. 3B). After distinguishing the upregulated differential nuclear proteins, we observed that metabolic pathways became more significant because more differential nuclear proteins in these pathways were detected after si-p97 treatment (Fig. 3C), suggesting that the loss of p97 makes substance metabolism more aberrant during this stage. For the nuclear proteins downregulated at 24 h (Fig. 3D and E), most pathways were related to DNA, indicating that DNA-related processes were not the primary task of the cells at this time. Among these pathways, four significantly changed in both the NM and NM + si-p97 groups; however, all were less significant in the presence of si-p97 (Fig. 3D). Other genes were quite different between the NM and NM + si-p97 groups (Fig. 3E), most of which were related to DNA damage repair, indicating different DNA repair responses.

3.4. P97 Regulates DNA Damage in NM Exposure

As shown in Fig. 3Aiv, we observed a significant increase in the total H2AX levels 24 h after NM + si-p97 treatment. Considering that the phosphorylation of H2AX is a crucial marker of DNA double strand break (DSB), we inferred that p97 plays a vital role in DNA damage repair. Given that more nuclear proteins can provide additional opportunities for crosslinking proteins to DNA, we compared the levels of DPC and H2AX with and without si-p97 intervention.

We found that exposure to NM led to DPC formation (Fig. 4A). DPCs were formed during the acute injury period after 1 h. To some extent, this may impede or delay the degradation of crosslinked proteins, obstructing protein export from the nucleus. However, compared to the NM group, the addition of si-p97 caused additional DPC formation at 24 h, but not at 1 h. This suggests that p97 is involved in DPC repair, specifically in the repair process after NM damage. Second, NM increased the levels of total-H2AX and p-H2AX levels. Si-p97 inhibited the increase in total-H2AX and p-H2AX at 1 h; however, it maintained high levels at 24 h (Fig. 4B and C).

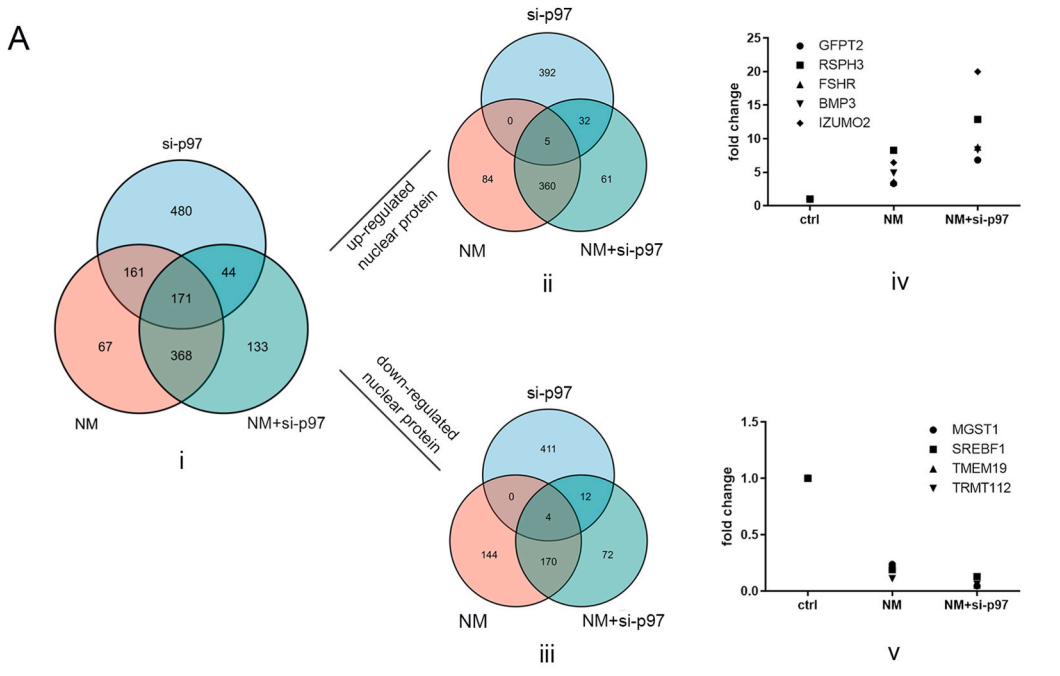

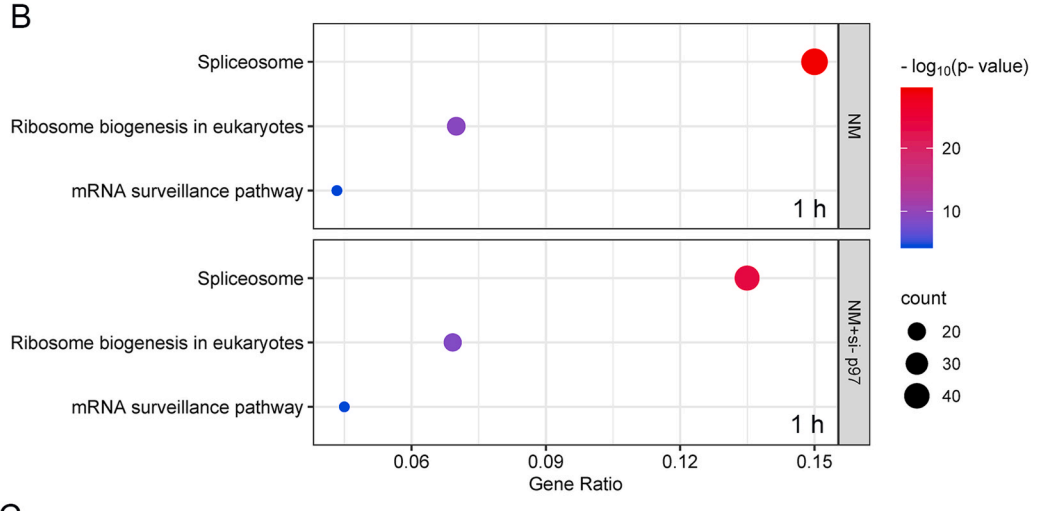

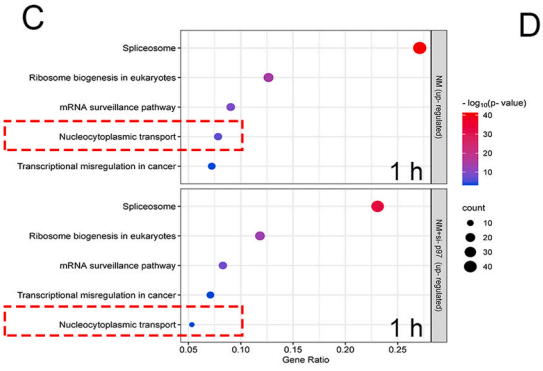

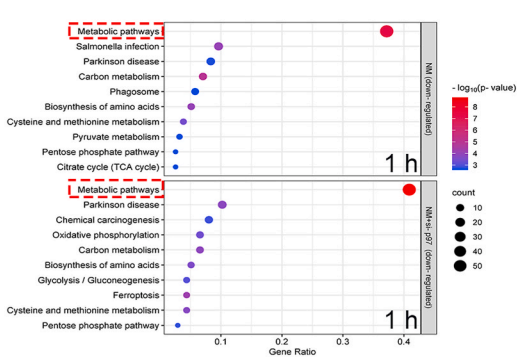

(caption on next page)

Fig. 2. Cluster analysis of differentially expressed nuclear protein 1 h after NM exposure and si-p97 intervention. (A) i: Venn diagram showing the results of pairwise comparisons of differentially expressed nuclear proteins between control, NM, and si-p97+NM groups at 1 h. ii-iii: Further categorization of proteins with differential expression at 1 h into upregulated and downregulated, represented by Venn diagrams; ii: Upregulated proteins; iii: Downregulated proteins. iv-v: Fold changes of proteins in the middle part of the Venn diagrams in ii and iii. (B) Clustering of all the differentially expressed nuclear proteins in NM and NM + si-p97 groups at 1 h using the KEGG database and the top 3 pathways were compared between the two groups. The x-axis represents the gene ratio, and the y-axis represents the pathway names. The color of the dots represents the p-value of the pathway, and the size of the dots represents the number of proteins enriched in that pathway. (C) Clustering of the upregulated nuclear proteins at 1 h in NM and si-p97+NM group, and the top 5 pathways were compared between the two groups. The representation methods are similar to B. (D) Clustering of the downregulated nuclear proteins at 1 h in NM and si-p97+NM group, and the top 10 pathways were compared between the two groups. The representation methods are similar to B.

3.5. Interaction between P97 and Proteasomes in NM Exposure

Considering that one function of p97 is to present proteins to proteasomes for degradation, we hypothesized that si-p97 would maintain high levels of nuclear protein content at 24 h and cause elevated DPC, which may be related to the inability of proteins to be transported to proteasomes. We investigated the damage caused by proteasome inhibition. Despite the high levels of p-H2AX produced by NM at 1 h, addition of the proteasome inhibitor MG132 partially prevented the increase in p-H2AX (Fig. 5A). MG132 showed a slight inhibitory effect on the NM-induced DPC removal after 24 h (Fig. 5B). These results were similar to those of si-p97 transfection, suggesting a synergistic interaction between p97 and proteasomes in NM damage and repair.

To identify the most active proteasomal components during NM and si-p97 treatment, we analyzed all subunits detected by LC-MS. At 1 h, 45 proteasome subunits were detected and at 24 h, 42 subunits were detected. Among all subunits, the expression of PSMD2 was the highest throughout the cell. Furthermore, the presence of si-p97 significantly increased the expression of PSMD2, as indicated by the dashed boxes in Fig. 5C and D.

Subsequently, the interaction between p97 and PSMD2 was analyzed by immunofluorescence staining. After NM treatment, the expression of PSMD2 was significantly upregulated and was mainly concentrated in the cell nucleus. Simultaneously, si-p97 intervention increased the content of PSMD2 in the cytoplasm (Fig. 5E–G). We speculate that more proteasomes are recruited to the cell nucleus to process unwanted proteins, such as those in DPC, and repair NM damage. Loss of p97 may partially reduce the nuclear loading of proteasomes and inhibit protein degradation.

3.6. Interaction between P97 and Protease DVC1 in Nuclear Protein Degradation

Previous studies have demonstrated the involvement of the protease DVC1, which interacts with p97, in DPC repair. We used GST-DVC1 to confirm the physical interaction between DVC1 and p97 (Fig. 6A), which is consistent with the findings of Davis [23]. To identify additional DVC1 partners, we used LC-MS to detect the proteins pulled down by GST-DVC1. Interestingly, in addition to p97, PSMD2 interacted with DVC1 (Supplemental Table 2). Therefore, we investigated the effects of DVC1 on PSMD2 and the proteasome. In the NM + si-DVC1 group, the expression of PSMD2 remained high, similar to that in the NM group; however, the content of PSMD2 in the cytoplasm increased (Fig. 6B–D), indicating that the absence of DVC1 failed to concentrate PSMD2 in the cell nucleus. After si-DVC1 treatment, proteasome activity decreased (Fig. 6E). Meanwhile, DPC formation significantly increased (Fig. 6F), similar to the effects observed with si-p97 or MG132 treatment. These data collectively demonstrate the collaboration of P97, DVC1, and proteasomes in the repair of DPC after NM damage.

4. Discussion

NM is considered a valuable material for military applications [24]. It induces tissue damage through various mechanisms possibly related to its molecular structure. Because of alkylation by its bifunctional groups, its targets extend beyond specific molecules to encompass a range of molecules with nucleophilic groups [25]. Consequently, essential cellular components, from DNA bases to proteins, can be directly or indirectly damaged. For instance, proteins can form DNA-protein crosslinks (DPC) under the influence of NM, leading to DNA damage. In contrast, damaged proteins and DPC can directly or indirectly disrupt cellular structure and function [26]. Therefore, understanding how changes in the proteome reflect cellular responses to nitrogen mustard damage is crucial.

This study used proteomics to understand cellular damage and repair globally. Additionally, two time points, 1 and 24 h, were selected. The 1-h time point reflects acute stress changes in cells after exposure to NM. In contrast, the 24-h time point reflects the repair process after a period of detachment from exposure, allowing for a more detailed assessment of the dynamic repair process. A significant change occurred in the nuclear protein spectrum and total amount during the acute injury phase. However, as time progressed, the total level of nuclear proteins and the number of differentially expressed proteins tended to return. The significantly involved pathways changed, indicating that severe damage occurs within the cell nucleus during acute exposure, which may be relieved or cause secondary stress during the removal stage of NM.

The primary functions of P97 include the removal of chromatin proteins, endoplasmic reticulum-mediated protein degradation, and membrane fusion [27,28]. P97 can capture target proteins and, relying on ATP hydrolysis, drive the target protein through its cycling domain, releasing the target protein from its original location (e.g., chromatin) [16,29]. Changes in the spatial structure of the target protein make it more susceptible to degradation [29]. Additionally, our previous study confirmed that p97 can remove MGMT proteins crosslinked with DNA [30].

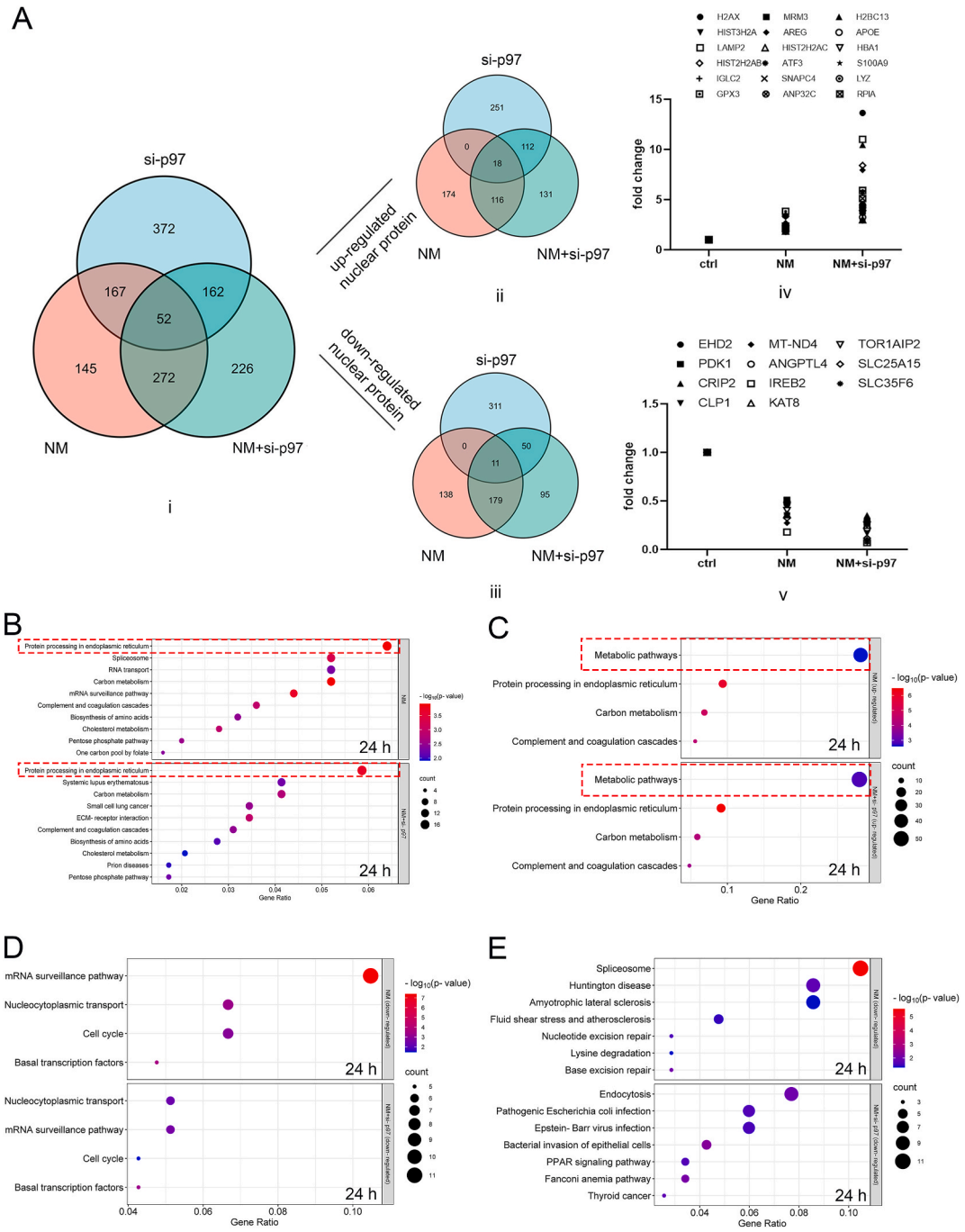

Fig. 3. Cluster analysis of differentially expressed nuclear protein 24 h after NM exposure and si-p97 intervention. (A) i: Venn diagram showing the results of pairwise comparisons of differentially expressed nuclear proteins between control, NM, and si-p97+NM groups at 24 h. ii-iii: Further categorization of proteins with differential expression at 24 h into upregulated and downregulated, represented by Venn diagrams; ii: Upregulated proteins; iii: Downregulated proteins. iv-v: Fold changes of proteins in the middle part of the Venn diagrams in ii and iii. (B) Clustering of all the differentially expressed nuclear proteins in NM and NM + si-p97 groups at 24 h using the KEGG database and the top 10 pathways were compared between the two groups. The x-axis represents the gene ratio, and the y-axis represents the pathway names. The color of the dots represents the p-value of the pathway, and the size of the dots represents the number of proteins enriched in that pathway. (C) Clustering of the upregulated nuclear proteins at 24 h in NM and si-p97+NM group, and the top 4 pathways were compared between the two groups. The representation methods are similar to B. (D) Clustering of the downregulated nuclear proteins at 24 h in NM and si-p97+NM group, and the same pathways involved in both groups are selected. The representation methods are similar to those of B. (E) Clustering of the downregulated nuclear proteins at 24 h in the NM and si-p97+NM groups, and the different pathways between the two groups are selected. Methods of representation are similar to B.

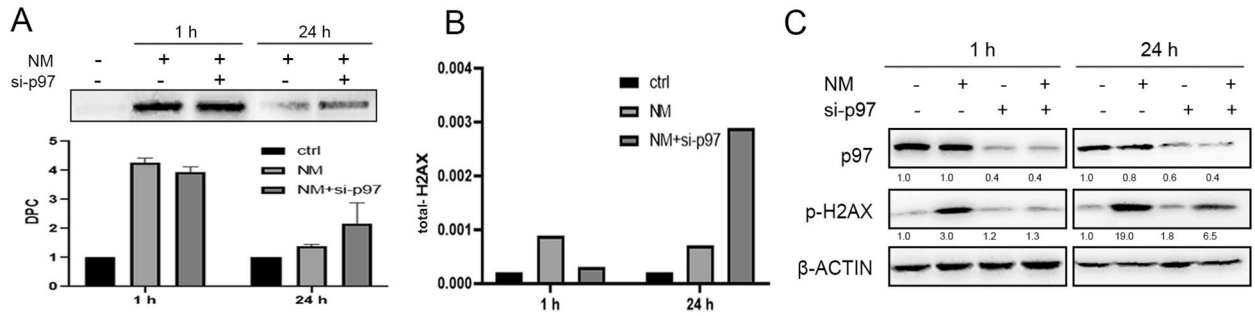

Fig. 4. Impact of NM and si-p97 on DPC formation and DSB. (A) DPC content after NM and si-p97 treatment at 1 and 24 h. (B) Relative expression levels of total-H2AX were detected by tandem mass spectrometry labeling at 1 h and 24 h in NM and NM + si-p97 groups. (C) Impact of NM and si-p97 on p-H2AX content at 1 and 24 h as detected by Western blot.

This study found that si-p97 did not result in severe DNA damage during acute exposure to NM (1 h), except for the weakening of nucleocytoplasmic transport. However, during the repair time (24 h), the types of differentially expressed nuclear proteins and the total amount of nuclear proteins in the NM + si-p97 group were greater than those in the NM group (Fig. 1C–E). Considering that the differentially expressed nuclear proteins partly reflect deviations from the normal state, no differential proteins should occur under normal conditions; this result suggests that p97 deletion may not be a primary factor exacerbating damage in the early exposure stage. However, the impact of p97 on nuclear proteins may manifest during the repair stage after NM withdrawal because a substantial number of nuclear proteins can be regulated by p97.

Proteomic cluster analysis revealed that during the acute injury phase, NM primarily influenced the upstream processes of cellular substance metabolism through several pathways, such as spliceosome, ribosome biogenesis, and mRNA surveillance (Fig. 2B). This may be attributed to DNA's early and rapid stress response to NM injury. The nucleocytoplasmic transport pathway was obstructed during the acute exposure due to p97 deficiency (Fig. 2C). At 24 h, an increase was observed in the different types of nuclear proteins and the total amount of nuclear proteins in the presence of si-p97, along with an increase in DPC (Fig. 1C–E, 4A), suggesting that the consequences of impeding nucleoplasmic transport during the acute injury phase may only become apparent at this time point, as it interferes with the export of proteins from the nucleus and promotes the formation of DPCs in subsequent stages. In addition, the activity of metabolism is significantly downregulated in the early stage of injury, which may be because the main response of cells at this time is concentrated upstream, such as nucleic acid-related events, or because the blockage of nucleocytoplasmic transport affects metabolism, which can be proven by the decrease in the activity of the metabolic pathway, which is more obvious when p97 is inhibited (Fig. 2D).

The signaling pathways involved in the repair stage are quite different from those involved in the early stage of injury. Interference during this period was mainly focused on protein processing in the endoplasmic reticulum and the downstream processes of specific metabolic pathways for various substances (Fig. 3B). Most downregulated proteins in Fig. 3Av were involved in metabolic processes. However, the metabolic pathway was the most significant pathway clustered by upregulated genes. This indicates complex metabolic regulation, including rescue and worse disruption at this time, which may be a delayed effect of acute DNA damage. The abnormality in endoplasmic reticulum protein processing suggests it is a predominant task in the nucleus at 24 h. It may also be metabolic-related; however, p97 deficiency reduced the number of enriched genes in this pathway (Fig. 3B). This is consistent with the results shown in Fig. 5, as PSMD2, a protein representing the endoplasmic reticulum protein processing pathway, was more highly expressed in the cytoplasm than in the nucleus when p97 was deficient. This suggests that p97 deficiency prevents the recruitment of molecules that deliver proteins to the endoplasmic reticulum, accumulating various proteins in the nucleus.

During the repair stage, nuclear-acid-related responses such as mRNA surveillance, cell cycle, and transcription were significantly downregulated, which may indicate that the main task of the cell shifts from early nucleic acid-related events to late metabolism-related events. However, si-p97 reduced these events to a lesser extent, suggesting that the nuclear acid-related response was still active (Fig. 3D and 4). Several downregulated pathways at this stage were DNA repair-related, such as nucleotide and base excision repair; both target less severe DNA damage, such as single-strand breaks. This downregulation may suggest that the DNA has been repaired or that these repairs are not the top choice. However, si-p97 inhibits the Fanconi anemia pathway, a repair method for DNA inter-strand crosslinking, and causes more severe damage (Fig. 3E). This suggests that p97 deletion may interfere with DNA repair in later stages, specifically the ability to repair severe damage. This was also evidenced by the long-term existence of DPC, total-H2AX, and p-H2AX, as shown in Fig. 6.

Various nuclear proteins play roles in DNA to ensure normal functions, including chromatin modeling, replication, transcription, and DNA repair. Typically, these proteins are recruited to DNA only briefly when needed and are released from DNA and protein complexes after completing their physiological functions. However, alkylating agents such as NM can cause stable covalent alkylation of DNA and proteins through their two N-chloroethyl groups, leading to the formation of DPC [31]. Our results confirmed that NM damage increased the DPC content (Fig. 4A). If the proteins on these DPCs were already present in the cell nucleus, they would only increase the DPC content, and there would not be an influx of proteins into the cell nucleus after 1 h. Therefore, our results suggest that proteins in the DPC inherently exist in the cell nucleus and also include some proteins that have already entered the cell nucleus but become crosslinked to the DNA chain upon contact with NM. This may be because NM can first undergo an addition reaction with a

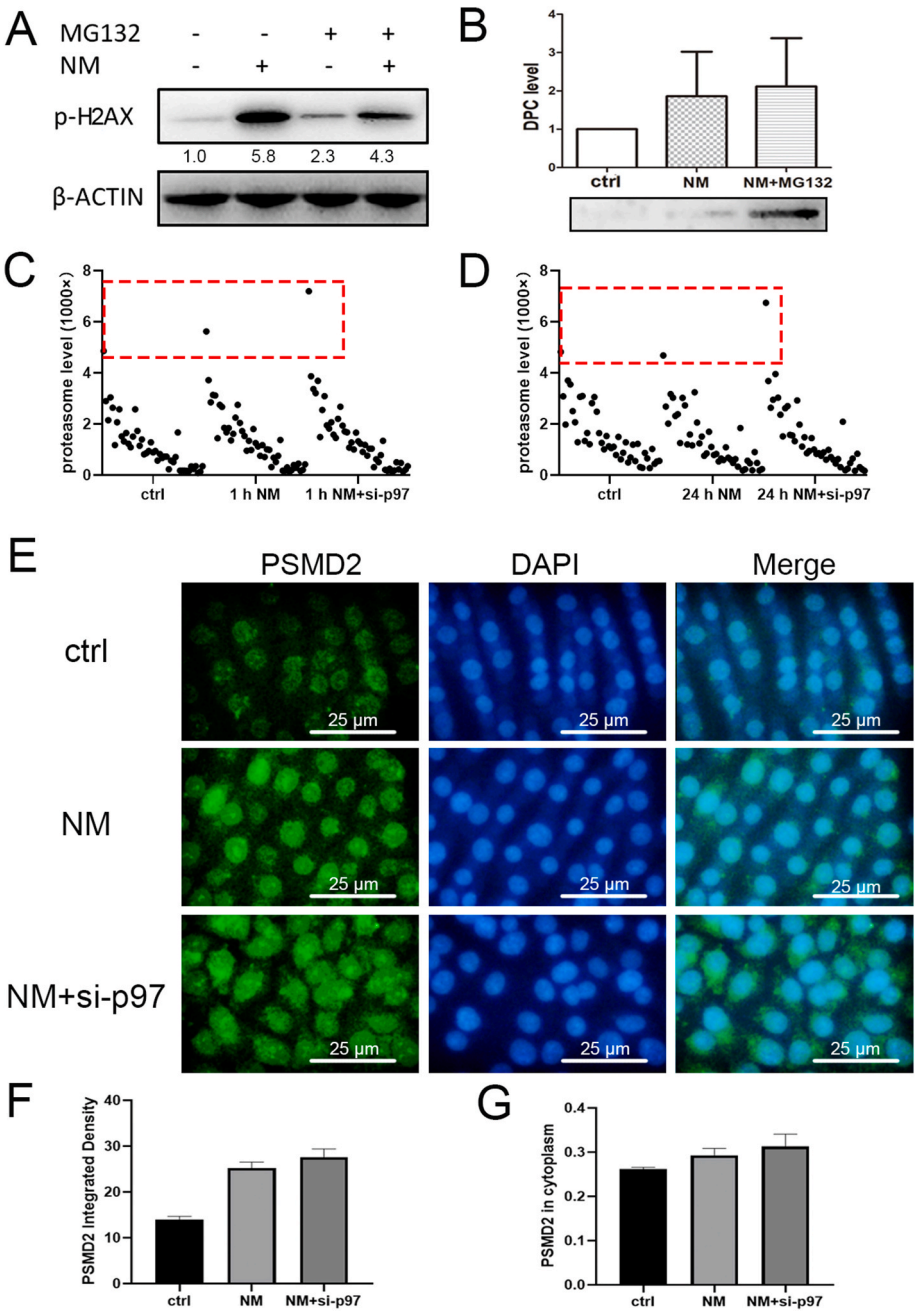

Fig. 5. Role of Proteasomes in NM-Induced Nuclear Damage. (A) Western blot detected p-H2AX content caused by NM and MG132 at 1 h. (B) Impact of NM and MG132 treatment on DPC content at 24 h. (C, D) Relative expression levels of proteasome subunits in different treatment groups at 1 or 24 h. PSMD2 is highlighted within the red dotted line. C: 1 h; D: 24 h. (E) Immunofluorescence staining of PSMD2. A scale bar of 25 μm is shown in figure. (F) The total fluorescence density of PSMD2 in E. (G) PSMD2 fluorescence intensity of cytoplasm relative to the nucleus in E.

protein containing one chloroethyl group, enter the cell nucleus with the protein from the addition reaction, and crosslink with the DNA chain containing another chloroethyl group.

Our data indicated that NM caused DNA DSB within 1 h, a severe form of DNA damage (marked by p-H2AX), which is consistent with previous reports [32] (Fig. 4C). However, the relationship between the various types of NM-induced DNA damage has not yet been experimentally validated. Our experiments revealed that NM induced both DPC and DSB within 1 h. However, when p97 was deleted, although DPC increased, the early (1-h) level of DSB did not increase significantly. After 24 h, DPC and DSB levels increased significantly, even without p97. Like H2AX, many upregulated proteins (Fig. 3Aii and iv) were histone-related proteins, which increased only at 24 h, probably due to the need for newly synthesized DNA. Based on its structure, NM can cause DPC or DNA chain

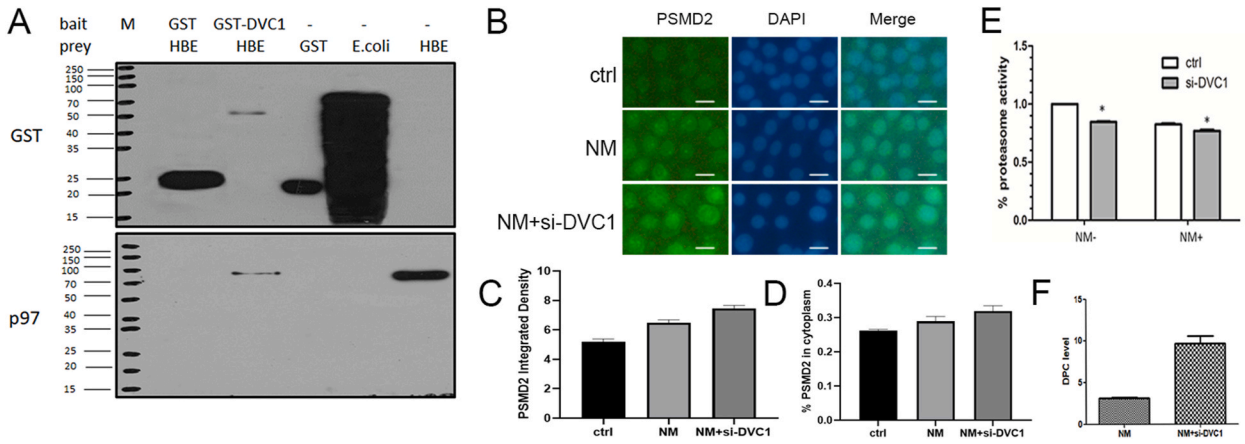

Fig. 6. Role of DVC1 via Proteasomes in Repairing NM-Induced DPC. (A) Interaction between DVC1 and p97. (B) PSMD2 content and location after treatment with NM or si-DVC1 combined. A scale bar of 5 μm is shown in figure. (C) The total fluorescence density of PSMD2 in B. (D) PSMD2 fluorescence intensity of cytoplasm relative to the nucleus in B. (E) Impact of si-DVC1 on proteasome activity. *, $P < 0.05$ vs. ctrl. (F) DPC levels after si-DVC1 treatment.

crosslinking through its two chloroethyl arms [33]; however, direct induction of DSB is unreasonable. We suspect that the increase in DSB within 1 h of NM treatment may be due to the replication pressure caused by DPC and DNA chain crosslinking. When p97 was deleted in the early stages (1 h), no more proteins entered the nucleus (Fig. 1E); therefore, the DPC level was not higher than that induced by NM alone (Fig. 4A), offsetting the impact on replication pressure and DSB formation to some extent (Fig. 4B and C) [34]. As time progressed, the deletion of p97 led to the aggregation of many proteins in the cell nucleus (Fig. 4A and 1C), and DPC could not be cleared. During DNA replication, owing to the continued presence of DPC, a large number of crosslinked proteins on the DNA chain lead to an increase in the replication pressure, causing DSB. This suggests that DSB are secondary phenomena in the progression of damage.

MG132, a proteasome inhibitor, inhibited p-H2AX levels in the early stages (Fig. 5A), similar to the results of si-p97 treatment, indicating that the proteasome inhibits protein entry into the cell nucleus in the early stages. However, proteasome inhibition also leads to a slower clearance of DPC [35]. Additionally, we observed an increase in PSMD2 levels after NM damage (Fig. 5C–E). PSMD2 is a subunit of the 26S proteasome ubiquitin receptor that participates in protein degradation during proteasomal function by encoding one of the non-ATPase subunits of the 19S regulatory subunit [36]. Moreover, elevated levels of PSMD2 expression may indicate the risk of abnormal cell proliferation and cell cycle progression, even predicting an unfavorable cancer prognosis [37,38]. Therefore, during NM damage, the concentration of PSMD2 near the nucleus may indicate genomic instability. However, when p97 was deleted, PSMD2 was dispersed throughout the cell, indicating that removing nuclear proteins was not the primary task, which is consistent with the results shown in Fig. 3D.

p97 interacts with ubiquitin ligases through its N-domain to recognize and transport multiple target proteins from the chromatin and endoplasmic reticulum to the cell membrane [27,39]. Our previous studies have confirmed that removing DNA-crosslinked MGMT protein depends on ubiquitination. Moreover, previous reports [40] have suggested that DVC1 is involved in presenting nuclear proteins to p97. DVC1 is involved in the degradation of target DNA proteins through its ubiquitin-binding domain [31]. Our experiments confirmed that DVC1 directly recognized p97 (Fig. 6A). Like p97, DVC1 can also bind to PSMD2; after DVC1 deletion, PSMD2 distribution tends to be throughout the entire cell rather than concentrated in the nucleus. Meanwhile, the activity of the proteasome decreased, and the DPC content increased, indicating that the inhibition of DVC1 also hinders the degradation of nuclear proteins through proteasomes (Supplemental Table 2, Fig. 6B and C). DVC1 may form a complex with p97 and the proteasome, participating in removing nuclear proteins. Based on the DVC1 and p97 domains, as well as the results of this study, we believe that p97's precise removal of specific nuclear proteins depends on DVC1.

In summary, this study found that NM causes a large influx of proteins into the cell nucleus and a significant change in the nuclear protein spectrum in the early stage, promoting the accumulation of DPC and causing DSB, resulting in the inhibition of replication, transcription, and translation, and ultimately disrupting energy metabolism. In addition, p97 facilitates the efflux of proteins from the cell nucleus and eliminates DPC, which plays a crucial role in cellular repair. The repair effects of p97 are closely related to the proteasome and DVC1. In this study, the process of p97's precise removal of specific nuclear proteins dependent on DVC1 was not thoroughly investigated and required further research.

Grant support

Young Talent Cultivation Program of Military Medical Science and Technology, PLA (grant number 20QNPY001); Talent Program of Chongqing Medical and Pharmaceutical College (grant number ygzrc2023105); Young Talent Cultivation Program of >Army Medical University (grant number 2018XQN03)

Data availability statement

Data will be made available on request.

CRediT authorship contribution statement

Jin Cheng: Writing – review & editing, Writing – original draft, Funding acquisition. **Haoyin Liu:** Data curation. **Wenpei Yu:** Data curation. **Xunhu Dong:** Methodology. **Yan Sai:** Project administration. **Feng Ye:** Methodology. **Guorong Dan:** Formal analysis. **Mingliang Chen:** Resources. **Yuanpeng Zhao:** Formal analysis. **Xi Zhang:** Supervision. **Zhongmin Zou:** Validation, Supervision.

Declaration of competing interest

The authors declare that they have no known competing financial interests or personal relationships that could have appeared to influence the work reported in this paper.

Appendix A. Supplementary data

Supplementary data to this article can be found online at https://doi.org/10.1016/j.heliyon.2024.e37401.

References

[1] S. Puyo, D. Montaudon, P. Pourquier, From old alkylating agents to new minor groove binders, Crit. Rev. Oncol.-Hematol. 89 (1) (2014) 43–61.
[2] G. Charkoftaki, J.V. Jester, D.C. Thompson, V. Vasiliou, Nitrogen mustard-induced corneal injury involves the sphingomyelin-ceramide pathway, Ocul. Surf. 16 (1) (2018) 154–162.
[3] J. Otter, J.L. D'Orazio, Blister Toxicity, Agents (mustard, vesicants, hd, hn1-3, H), in: *StatPearls*. Treasure Island (FL), StatPearls Publishing StatPearls Publishing LLC, 2018.
[4] K. Liner, C. Brown, L.Y. McGirt, Clinical potential of mechlorethamine gel for the topical treatment of mycosis fungoides-type cutaneous T-cell lymphoma: a review on current efficacy and safety data, Drug Des. Dev. Ther. 12 (2018) 241–254.
[5] O. Larrañaga, A. de Cózar, F.P. Cossío, Mono- and di-alkylation processes of DNA bases by nitrogen mustard mechlorethamine, ChemPhysChem : a European journal of chemical physics and physical chemistry 18 (23) (2017) 3390–3401.
[6] R. Loeber, E. Michaelson, Q. Fang, C. Campbell, A.E. Pegg, N. Tretyakova, Cross-linking of the DNA repair protein Omicron6-alkylguanine DNA alkyltransferase to DNA in the presence of antitumor nitrogen mustards, Chem. Res. Toxicol. 21 (4) (2008) 787–795.
[7] A. Romero, E. Ramos, F. Lopez-Munoz, C. De Los Rios, J. Egea, E. Gil-Martin, R. Pita, J.J. Torrado, D.R. Serrano, A. Juberias, Toxicology of blister agents: is melatonin a potential therapeutic option? Diseases 9 (2) (2021).
[8] At Groehler, P.W. Villalta, C. Campbell, N. Tretyakova, Covalent DNA-protein cross-linking by phosphoramide mustard and nornitrogen mustard in human cells, Chem. Res. Toxicol. 29 (2) (2016) 190–202.
[9] M.H. Trager, C. Chen, S. Husain, L.J. Geskin, Nitrogen mustard gel-induced inflammation triggers lymphomatoid papulosis in patients with mycosis fungoides, The Journal of dermatology 47 (5) (2020) 546–550.
[10] X. Dong, Y. He, F. Ye, Y. Zhao, J. Cheng, J. Xiao, W. Yu, J. Zhao, Y. Sai, G. Dan, et al., Vitamin D3 ameliorates nitrogen mustard-induced cutaneous inflammation by inactivating the NLRP3 inflammasome through the SIRT3-SOD2-mtROS signaling pathway, Clin. Transl. Med. 11 (2) (2021) e312.
[11] L. Au, J.P. Meisch, L.M. Das, A.M. Binko, R.S. Boxer, A.M. Wen, N.F. Steinmetz, K.Q. Lu, Suppression of hyperactive immune responses protects against nitrogen mustard injury, J. Invest. Dermatol. 135 (12) (2015) 2971–2981.
[12] R. Malaviya, A. Bellomo, E. Abramova, C.R. Croutch, J. Roseman, R. Tuttle, E. Peters, R.P. Casillas, V.R. Sunil, J.D. Laskin, et al., Pulmonary injury and oxidative stress in rats induced by inhaled sulfur mustard is ameliorated by anti-tumor necrosis factor-alpha antibody, Toxicol. Appl. Pharmacol. 428 (2021) 115677.
[13] D. Kumar, N. Tewari-Singh, C. Agarwal, A.K. Jain, S. Inturi, R. Kant, C.W. White, R. Agarwal, Nitrogen mustard exposure of murine skin induces DNA damage, oxidative stress and activation of MAPK/Akt-AP1 pathway leading to induction of inflammatory and proteolytic mediators, Toxicology letters 235 (3) (2015) 161–171.
[14] N.L. Klages-Mundt, L. Li, Formation and repair of DNA-protein crosslink damage, Sci. China Life Sci. 60 (10) (2017) 1065–1076.
[15] B. Vaz, M. Popovic, K. Ramadan, DNA-protein crosslink proteolysis repair, Trends Biochem. Sci. 42 (6) (2017) 483–495.
[16] P. Hanzelmann, H. Schindelin, The Interplay of Cofactor interactions and post-translational modifications in the regulation of the AAA+ ATPase p97, Front. Mol. Biosci. 4 (2017) 21.
[17] D.M. Huryn, D.J.P. Kornfilt, P. Wipf, p97: an emerging target for cancer, neurodegenerative diseases, and viral infections, J. Med. Chem. 63 (5) (2020) 1892–1907.
[18] J. Rageul, A.S. Weinheimer, J.J. Park, H. Kim, Proteolytic control of genome integrity at the replication fork, DNA Repair (2019) 102657.
[19] K. Kiianitsa, N. Maizels, A rapid and sensitive assay for DNA-protein covalent complexes in living cells, Nucleic Acids Res. 41 (9) (2013) e104.
[20] F. Busi, Fluorescent oligonucleotide probes for the quantification of RNA by real-time qPCR, Methods Mol. Biol. 2113 (2020) 263–280.
[21] M.I. Shoulkamy, T. Nakano, M. Ohshima, R. Hirayama, A. Uzawa, Y. Furusawa, H. Ide, Detection of DNA-protein crosslinks (DPCs) by novel direct fluorescence labeling methods: distinct stabilities of aldehyde and radiation-induced DPCs, Nucleic Acids Res. 40 (18) (2012) e143.
[22] B.M. Bolstad, R.A. Irizarry, M. Astrand, T.P. Speed, A comparison of normalization methods for high density oligonucleotide array data based on variance and bias, Bioinformatics 19 (2) (2003) 185–193.
[23] E.J. Davis, C. Lachaud, P. Appleton, T.J. Macartney, I. Nathke, J. Rouse, DVC1 (C1orf124) recruits the p97 protein segregase to sites of DNA damage, Nat. Struct. Mol. Biol. 19 (11) (2012) 1093–1100.
[24] K. Ghabili, P.S. Agutter, M. Ghanei, K. Ansarin, M.M. Shoja, Mustard gas toxicity: the acute and chronic pathological effects, J. Appl. Toxicol. 30 (7) (2010) 627–643.
[25] D. Steinritz, R. Luling, M. Siegert, J. Herbert, H. Muckter, C.D. Taeger, T. Gudermann, A. Dietrich, H. Thiermann, H. John, Alkylated epidermal creatine kinase as a biomarker for sulfur mustard exposure: comparison to adducts of albumin and DNA in an in vivo rat study, Arch. Toxicol. 95 (4) (2021) 1323–1333.
[26] L. Yue, Y. Wei, J. Chen, H. Shi, Q. Liu, Y. Zhang, J. He, L. Guo, T. Zhang, J. Xie, et al., Abundance of four sulfur mustard-DNA adducts ex vivo and in vivo revealed by simultaneous quantification in stable isotope dilution-ultrahigh performance liquid chromatography-tandem mass spectrometry, Chem. Res. Toxicol. 27 (4) (2014) 490–500.
[27] L. Stach, P.S. Freemont, The AAA+ ATPase p97, a cellular multitool, Biochem. J. 474 (17) (2017) 2953–2976.

[28] M. Kustermann, L. Manta, C. Paone, J. Kustermann, L. Lausser, C. Wiesner, L. Eichinger, C.S. Clemen, R. Schroder, H.A. Kestler, et al., Loss of the novel Vcp (valosin containing protein) interactor Washc4 interferes with autophagy-mediated proteostasis in striated muscle and leads to myopathy in vivo, Autophagy 14 (11) (2018) 1911–1927.
[29] N. Bodnar, T. Rapoport, Toward an understanding of the Cdc48/p97 ATPase, F1000Research 6 (2017) 1318.
[30] J. Cheng, F. Ye, G. Dan, Y. Zhao, B. Wang, J. Zhao, Y. Sai, Z. Zou, Bifunctional alkylating agent-mediated MGMT-DNA cross-linking and its proteolytic cleavage in 16HBE cells, Toxicol. Appl. Pharmacol. 305 (2016) 267–273.
[31] M. Morocz, E. Zsigmond, R. Toth, M.Z. Enyedi, L. Pinter, L. Haracska, DNA-dependent protease activity of human Spartan facilitates replication of DNA-protein crosslink-containing DNA, Nucleic Acids Res. 45 (6) (2017) 3172–3188.
[32] Y.H. Jan, D.E. Heck, D.L. Laskin, J.D. Laskin, DNA damage signaling in the cellular responses to mustard vesicants, Toxicology letters 326 (2020) 78–82.
[33] R.K. Singh, S. Kumar, D.N. Prasad, T.R. Bhardwaj, Therapeutic journery of nitrogen mustard as alkylating anticancer agents: historic to future perspectives, Eur. J. Med. Chem. 151 (2018) 401–433.
[34] R.L. Swan, I.G. Cowell, C.A. Austin, A role for VCP/p97 in the processing of drug-stabilised TOP2-DNA covalent complexes, Mol. Pharmacol. 100 (1) (2021) 57–62.
[35] S. Ortega-Atienza, S.E. Green, A. Zhitkovich, Proteasome activity is important for replication recovery, CHK1 phosphorylation and prevention of G2 arrest after low-dose formaldehyde, Toxicol. Appl. Pharmacol. 286 (2) (2015) 135–141.
[36] K. Ying, C. Wang, S. Liu, Y. Kuang, Q. Tao, X. Hu, Diverse Ras-related GTPase DIRAS2, downregulated by PSMD2 in a proteasome-mediated way, inhibits colorectal cancer proliferation by blocking NF-kappaB signaling, Int. J. Biol. Sci. 18 (3) (2022) 1039–1050.
[37] Y. Li, J. Huang, B. Zeng, D. Yang, J. Sun, X. Yin, M. Lu, Z. Qiu, W. Peng, T. Xiang, et al., PSMD2 regulates breast cancer cell proliferation and cell cycle progression by modulating p21 and p27 proteasomal degradation, Cancer Lett. 430 (2018) 109–122.
[38] A. Salah Fararjeh, A. Al-Khader, M. Al-Saleem, R. Abu Qauod, The prognostic significance of proteasome 26S subunit, non-ATPase (PSMD) genes for bladder urothelial carcinoma patients, Cancer Inform 20 (2021) 11769351211067692.
[39] F. Limanaqi, C.L. Busceti, F. Biagioni, F. Cantini, P. Lenzi, F. Fornai, Cell-clearing systems bridging Repeat expansion proteotoxicity and neuromuscular junction alterations in ALS and SBMA, Int. J. Mol. Sci. 21 (11) (2020) 4021.
[40] A. Mosbech, I. Gibbs-Seymour, K. Kagias, T. Thorslund, P. Beli, L. Povlsen, S.V. Nielsen, S. Smedegaard, G. Sedgwick, C. Lukas, et al., DVC1 (C1orf124) is a DNA damage-targeting p97 adaptor that promotes ubiquitin-dependent responses to replication blocks, Nat. Struct. Mol. Biol. 19 (11) (2012) 1084–1092.